The Astrophysical Journal, 658:65–77, 2007 March 20


# THE IMPORTANCE OF DRY AND WET MERGING ON THE FORMATION AND EVOLUTION OF ELLIPTICAL GALAXIES

L. Ciotti,[1] B. Lanzoni,[2] and M. Volonteri[3]
*Received 2006 September 7; accepted 2006 November 9*


## ABSTRACT

With the aid of a simple yet robust approach, we investigate the influence of dissipationless and dissipative merging on galaxy structure and the consequent effects on the scaling laws followed by elliptical galaxies. Our results suggest that elliptical galaxies cannot be originated by parabolic merging of low-mass spheroids only, even in the presence of substantial gas dissipation. However, we also found that scaling laws such as the Faber-Jackson, Kormendy, fundamental plane, and $M_{\rm BH}$-$\sigma$ relations, when considered over the whole mass range spanned by elliptical galaxies in the local universe, are robust against merging. We conclude that galaxy scaling laws, possibly established at high redshift by the fast collapse in preexisting dark matter halos of gas-rich and clumpy stellar distributions, are compatible with a (small) number of galaxy mergers at lower redshift.


*Subject headings:* galaxies: elliptical and lenticular, cD — galaxies: evolution — galaxies: formation — galaxies: fundamental parameters — galaxies: structure

## 1. INTRODUCTION

Early-type galaxies are known to follow well-defined empirical scaling laws that relate their global observational properties, such as the total luminosity $L$, the effective radius $R_e$, and the central velocity dispersion $\sigma$, to one another. Among other laws, we recall the Faber-Jackson (FJ; Faber & Jackson 1976), Kormendy (1977), fundamental plane (FP; Djorgovski & Davis 1987; Dressler et al. 1987), color-$\sigma$ (Bower et al. 1992), and $\mathrm{Mg}_2$-$\sigma$ (e.g., Guzmán et al. 1992; Bernardi et al. 2003c) relations. In addition, it is now believed that all elliptical galaxies host a central supermassive black hole (SMBH; e.g., see de Zeeuw 2001), whose mass $M_{\rm BH}$ scales with the stellar mass $M_*$ and velocity dispersion $\sigma$ of the host galaxy (Magorrian et al. 1998; Ferrarese & Merritt 2000; Gebhardt et al. 2000; Tremaine et al. 2002). Clearly, these scaling relations provide invaluable information about the formation and evolution of early-type galaxies and set stringent constraints to galaxy formation models.

The two major formation models for elliptical galaxies that have been proposed so far are the monolithic (Eggen et al. 1962) and merging (Toomre 1977; White & Frenk 1991) scenarios. Each of them has observational and theoretical successes and drawbacks (e.g., see Ostriker 1980; McIntosh et al. 2005; Renzini 2006). For instance, we list here three observational and theoretical pieces of evidence in favor of a fast and dissipative monolithic collapse.

First, the observed color-magnitude and $\mathrm{Mg}_2$-$\sigma$ relations, as well as the increase of the $[\alpha/\mathrm{Fe}]$ ratio with $\sigma$ in the stellar population of elliptical galaxies (e.g., see Jørgensen 1999; Thomas et al. 1999; Saglia et al. 2000; Bernardi et al. 2003c and references therein), suggest that star formation in massive elliptical galaxies was not only more efficient than that in low-mass galaxies, but also that it was a faster process (i.e., completed before Type Ia supernova explosions take place), with timescales of gas consumption and ejection that are shorter than or comparable to the galaxy dynamical time (e.g., see Matteucci 1994; Pipino & Matteucci 2004) and decrease for increasing galaxy mass.

Second, the structural and dynamical properties of elliptical galaxies are well reproduced by cold dissipationless collapse, a process that is expected to dominate the last stages of highly dissipative collapses, in which the gas cooling time of the forming galaxy is shorter than its dynamical time, so that stars form "in flight," and the subsequent dynamical evolution is a dissipationless collapse. It is now well established that the end products of cold and phase-space clumpy collapses have projected density profiles that are well described by the $R^{1/4}$ de Vaucouleurs (1948) law, radially decreasing line-of-sight velocity dispersion profiles, and radially increasing velocity anisotropies, in agreement with what is observed in elliptical galaxies (e.g., see van Albada 1982; May & van Albada 1984; McGlynn 1984; Aguilar & Merritt 1990; Londrillo et al. 1991; Udry 1993; Hozumi et al. 2000; Trenti et al. 2005).

Third, the current and remarkably successful cosmological scenario for structure formation predicts that well-defined scaling laws are imprinted in the dark matter (DM) halos; in particular, the virial velocity dispersion of DM halos increases as $\sigma_v \propto M_{\rm DM}^{1/3}$. This is because virialized DM halos are the *collapse* end products of negative energy (inhomogeneous) density distributions, in which the absolute value of the binding energy per unit mass increases with the halo mass (Peebles 1980). On the contrary, in a parabolic merging, $\sigma_v$ would not increase with halo mass.

Thus, the observed scaling laws of elliptical galaxies could be originated by the fast collapse of inhomogeneous gas and star distributions in preexisting DM halos, rather than by parabolic merging processes (e.g., see Lanzoni et al. 2004). Note that high-resolution $N$-body simulations (Nipoti et al. 2006) have shown that cold (dissipationless) collapses in preexisting DM halos nicely reproduce the weak homology of elliptical galaxies (e.g., see Caon et al. 1993; Prugniel & Simien 1997; Bertin et al. 2002, hereafter BCD02; Graham & Guzmán 2003) and the central break radius in their surface brightness profile (Ferrarese et al. 1994; Lauer et al. 1995; Graham et al. 2003; Trujillo et al. 2004).

The last point above is particularly puzzling because the available observations seem to indicate that mergers may happen in the life of elliptical galaxies, with dissipative (wet) mergers dominating at high redshift and gas-free (dry) merging mainly affecting massive elliptical galaxies at $z \lesssim 1.5$ (e.g., see Khochfar & Burkert 2003; Bell et al. 2004, 2006; van Dokkum 2005; Faber

[1] Dipartimento di Astronomia, Università di Bologna, Bologna, Italy.
[2] INAF–Osservatorio Astronomico di Bologna, Bologna, Italy.
[3] Institute of Astronomy, University of Cambridge, Cambridge, UK.

et al. 2005; Conselice 2006). This picture is also suggested by the available information on the star formation history of the universe and the redshift evolution of the quasar luminosity function (see, e.g., Haehnelt & Kauffmann 2000; Burkert & Silk 2001; Yu & Tremaine 2002; Cavaliere & Vittorini 2002; Haiman et al. 2004). In addition, parabolic orbits seem to be quite relevant in the hierarchical merging picture (e.g., see Benson 2005; Khochfar & Burkert 2006). To get insight on this issue, in the present paper we will focus on the remarkable homogeneity and regularity of the family of early-type galaxies (as testified by their scaling laws), and we explore the consequences of galaxy merging on them.

The impact of dry merging on the scaling laws of early-type galaxies has been already investigated in several works (e.g., Capelato et al. 1995; Pentericci et al. 1996; Haehnelt & Kauffmann 2000; Ciotti & van Albada 2001, hereafter CvA01; Evstigneeva et al. 2002; Nipoti et al. 2003, hereafter NLC03; González-García & van Albada 2003; Dantas et al. 2003; Evstigneeva et al. 2004; Boylan-Kolchin et al. 2005, 2006). In particular, the simple approach of CvA01 and the *N*-body simulations of NLC03 showed that repeated, parabolic merging of gas-free galaxies is unable to reproduce the observed scaling laws, because the merger products are characterized by an unrealistically large effective radius and a mass-independent velocity dispersion (see also Shen et al. 2003). However, simple physical arguments show that gas dissipation should be able to mitigate the problems posed by dry merging to the explanation of the observed scaling laws (e.g., see CvA01; Kazantzidis et al. 2005; Robertson et al. 2006a, 2006b; Dekel & Cox 2006).[4] Unfortunately, numerical simulations with gas dissipation are considerably more complicated than pure *N*-body simulations (e.g., see Sáiz et al. 2004; Oñorbe et al. 2005, 2006; Tissera et al. 2006; Robertson et al. 2006a, 2006b), and in particular, very few of them have been made using realistic cosmological initial conditions (e.g., see Naab et al. 2007 and references therein). For these reasons, by generalizing the approach presented in CvA01 to the dissipative case, we further investigate with Monte Carlo simulations the compatibility of galaxy merging with the formation and evolution of early-type galaxies, focusing in particular on (1) the effects of gas dissipation on the merger end products (wet merging) and (2) the effects of parabolic dry and wet merging on the scaling laws that elliptical galaxies follow in the local universe. We argue that parabolic merging of low-mass seed galaxies alone cannot be at the origin of the scaling laws, even though wet mergers lead to early-type galaxies that follow the observed scaling laws better than the end products of dry merging. We also show that galaxy scaling laws, such as the FJ, Kormendy, and FP relations, once in place, are robust against merging. Thus, our results reinforce the idea that monolithic collapse at early times and subsequent merging could just represent the different phases of galaxy formation (collapse) and evolution (merging, in addition to the aging of the stellar populations and related phenomena; e.g., see Khochfar & Silk 2006; Naab et al. 2006).

This paper is organized as follows. In § 2 we derive the recursive equations describing the evolution of galaxy properties after dry and wet parabolic mergers, and we discuss in detail the case of equal-mass merging. In § 3 we use the derived relations in Monte Carlo investigations of merging of elliptical galaxy populations, and the main results are finally summarized and discussed in § 4.

[4] Note that by comparing the FP of galaxies and that of galaxy clusters, Burstein et al. (1997) and Lanzoni et al. (2004) suggested that, at variance with groups and clusters, gas dissipation must have had an important role on the formation and evolution of elliptical galaxies.

## 2. THE MODELS

In this section we now derive from elementary physics arguments the relations between the properties of the progenitor galaxies and the properties of the merging end products that will be used in the rest of the paper. For simplicity, in the adopted scheme each elliptical galaxy is modeled as a nonrotating, isotropic, and spherically symmetric virialized system, characterized by a stellar mass $M_*$, a gas mass $M_g = \alpha M_*$, and a SMBH mass $M_{\rm BH} = \mu M_*$; from observations, $\mu \simeq 10^{-3}$ in $z = 0$ spheroids (Magorrian et al. 1998). In our treatment we do not consider the presence of a DM halo, as it could be introduced just by rescaling the model stellar mass-to-light ratio if the DM density distribution is proportional to the stellar one, as discussed in the following paragraphs. The total energy of a galaxy is then given by

$$E = K_* + U_g + W, \tag{1}$$

where

$$K_* = \frac{3}{2}\int \rho_* \sigma_*^2 \, dV \tag{2}$$

is the stellar kinetic energy and

$$U_g = \frac{3k_{\rm B}}{2\langle m\rangle}\int \rho_g T \, dV \tag{3}$$

is the gas internal energy; $\sigma_*$, $k_{\rm B}$, $T$, and $\langle m\rangle$ are the stellar one-dimensional velocity dispersion, the Boltzmann constant, the gas temperature, and the gas mean molecular mass, respectively. Finally,

$$W = \frac{1}{2}\int (\rho_* + \rho_g)(\phi_* + \phi_g)\, dV \tag{4}$$

is the total gravitational energy of stars and gas (we do not consider the negligible contribution of the central SMBH).

Under the simplifying assumption that the gas is spatially distributed proportionally to the stellar distribution (i.e., $\rho_g = \alpha\rho_*$), then $\phi_g = \alpha\phi_*$, and

$$W = (1+\alpha)^2 W_*, \tag{5}$$

where $W_*$ is the self-gravitational energy of the stellar component. Furthermore, if we assume that the gas is in equilibrium in the total gravitational field, from the Jeans and the hydrostatic equations, it results that $T = \langle m\rangle\sigma_*^2/k_{\rm B}$, and from equations (2)–(3),

$$U_g = \alpha K_*. \tag{6}$$

Finally, from equations (5)–(6) and the virial theorem for the two-component system of stars and gas, the total galactic energy can be written in terms of the stellar energy and of the relative amount of gas as

$$E = -(1+\alpha)K_* = \frac{(1+\alpha)^2}{2} W_*. \tag{7}$$

Note that a DM halo of mass $M_{\rm DM} = \alpha_{\rm DM} M_*$ distributed proportionally to the stellar distribution would be easily considered in the present scheme by the addition of a new parameter $\alpha_{\rm DM}$ in equations (5)–(7).

The quantities introduced so far are not directly observable, and so in § 2.1 we will show how to relate the characteristic

one-dimensional stellar velocity dispersion $\sigma_v$ and the characteristic radius $r_v$, defined as

$$K_* \equiv \frac{3}{2} M_* \sigma_v^2, \tag{8}$$

$$|W_*| \equiv \frac{GM_*^2}{r_v}, \tag{9}$$

to the galaxy effective radius $R_e$ and the central projected velocity dispersion $\sigma$.[5]

We now focus on the parabolic merging of two galaxies, so that the total energy of the system is the sum of the internal potential and kinetic energies of the two progenitor galaxies; we also assume that no mass is lost in the process. During the merging, as a consequence of gas dissipation, a fraction $\eta$ of the available gas mass is converted into stars, and the stellar mass balance equation is

$$M_* = M_{*1} + M_{*2} + \eta(M_{g1} + M_{g2}). \tag{10}$$

Furthermore, a new SMBH forms by the coalescence of the two central black holes (BHs) and a fraction $f\eta$ of the available gas is accreted on it, leading to a BH of final mass

$$M_{\rm BH} = (M_{\rm BH1}^p + M_{\rm BH2}^p)^{1/p} + f\eta(M_{g1} + M_{g2}). \tag{11}$$

The free parameter $1 \le p \le 2$ describes how much BH rest mass is radiated as gravitational waves during the BH coalescence: $p = 1$ corresponds to the classical merging case (no gravitational radiation), while $p = 2$ corresponds to the maximally radiative case for nonrotating BHs. Note that in equation (11) it is implicitly assumed that first $M_{\rm BH1}$ and $M_{\rm BH2}$ merge, and then the gas is accreted on the new BH; the other extreme case would be that of gas accretion followed by merging (e.g., see Hughes & Blandford 2003). Of course, if $p = 1$, there is no difference in the final mass; in the Monte Carlo simulations described in § 3, we explored both cases, finding no significant differences. As a consequence of star formation and BH accretion, the gas mass balance equation is

$$M_g = (1 - \eta - f\eta)(M_{g1} + M_{g2}), \tag{12}$$

which implies that $0 \le \eta \le 1/(1 + f)$. Thus, the gas-to-star mass ratio after the merger and the new Magorrian coefficient, respectively, are given by

$$\alpha \equiv \frac{M_g}{M_*} = \frac{(1 - \eta - f\eta)(\alpha_1 M_{*1} + \alpha_2 M_{*2})}{(1 + \eta\alpha_1)M_{*1} + (1 + \eta\alpha_2)M_{*2}}, \tag{13}$$

$$\mu \equiv \frac{M_{\rm BH}}{M_*} = \frac{(\mu_1^p M_{*1}^p + \mu_2^p M_{*2}^p)^{1/p} + f\eta(\alpha_1 M_{*1} + \alpha_2 M_{*2})}{(1 + \eta\alpha_1)M_{*1} + (1 + \eta\alpha_2)M_{*2}}. \tag{14}$$

Note that if $p = 1$ and $f = \mu_1 = \mu_2$, the proportionality coefficient $\mu$ remains unchanged after the merging; also note that the scheme above is generalizable by allowing for different values of $f$ and $\eta$ in the two progenitor galaxies, but for simplicity in this paper we assume that $f$ and $\eta$ are fixed.

In order to describe the effects on $r_v$ and $\sigma_v$ of the radiative energy losses associated with gas dissipation, a fraction $(1 + f)\eta$ of the gas internal energy $U_g$ of each progenitor is subtracted from the total energy budget of the merger product, consistent with the previous assumptions.[6] Thus, from equation (6), the final total energy of the remnant is

$$E = E_1 + E_2 - \eta(1 + f)(\alpha_1 K_{*1} + \alpha_2 K_{*2}). \tag{15}$$

The new total energy $E$, the new mass ratio $\alpha$, and the new total stellar mass $M_*$ are given by equations (15), (13), and (10), respectively. From equation (7) it follows that for the new galaxy,

$$\sigma_v^2 = \frac{M_{*1} + M_{g1}}{M_* + M_g} A_1 \sigma_{v1}^2 + \frac{M_{*2} + M_{g2}}{M_* + M_g} A_2 \sigma_{v2}^2, \tag{16}$$

$$\frac{1}{r_v} = \left(\frac{M_{*1} + M_{g1}}{M_* + M_g}\right)^2 \frac{A_1}{r_{v1}} + \left(\frac{M_{*2} + M_{g2}}{M_* + M_g}\right)^2 \frac{A_2}{r_{v2}}, \tag{17}$$

$$A_1 = 1 + \frac{(1 + f)\eta\alpha_1}{1 + \alpha_1}, \tag{18}$$

and a similar expression holds for $A_2$. In a dry ($\eta = 0$) merging, $A_1 = A_2 = 1$, so that

$$\min(\sigma_{v1}^2, \sigma_{v2}^2) \le \sigma_v^2 = \frac{(1 + \alpha_1)M_{*1}\sigma_{v1}^2 + (1 + \alpha_2)M_{*2}\sigma_{v2}^2}{(1 + \alpha_1)M_{*1} + (1 + \alpha_2)M_{*2}} \le \max(\sigma_{v1}^2, \sigma_{v2}^2); \tag{19}$$

that is, the virial velocity dispersion of the merger product cannot be larger than the maximum velocity dispersion of the progenitors (the $\alpha > 0$ and $\eta = 0$ case also describes the situation in which the gaseous component is replaced by a DM halo). Instead, $A > 1$ in the case of wet ($\eta > 0$) merging, and the resulting $\sigma_v$ is larger than in the dry case and possibly larger than the maximum velocity dispersion of the progenitors. A similar argument shows that in the presence of gas dissipation, the new $r_v$ increases less than in the dry case. Note that the conclusions of this preparatory analysis are obtained under the hypothesis of parabolic merging. If mergers involve galaxies on bound orbits, the additional negative energy term in equation (15) would lead to an increase of $\sigma_v$ in equal-mass dry mergers as well. The analysis of this case, and the question of how fine-tuned the properties of the progenitor galaxies should be with their binding orbital energy in order to reproduce the scaling laws, are not further discussed in this paper (e.g., see Boylan-Kolchin et al. 2005, 2006; Almeida et al. 2007).

### 2.1. *Relating Intrinsic and Observational Properties: Weak Homology Effects*

So far the discussion has involved galaxy virial properties only. However, galaxy scaling laws relate observational quantities such as the total luminosity $L$, the central projected velocity dispersion $\sigma$ (luminosity averaged over some aperture), and the circularized effective radius $R_e$. For example, in this paper we compare our models with the FJ [$L \propto \sigma^{3.92}$, rms$(\log \sigma) = 0.075$], Kormendy [$L \propto R_e^{1.58}$, rms$(\log R_e) = 0.1$], and edge-on FP[7]

[5] Note that $\sigma_v$ and $r_v$ in eqs. (8) and (9) coincide with the virial velocity dispersion and the virial radius of the star+gas system. This would not be true in a system in which $\rho_* \neq \rho_g$.

[6] This represents the limiting case where energy losses affect the internal energies of the progenitor galaxies *before* they merge. In the other limiting case the two galaxies would merge without dissipation, and then a fraction $(1 + f)\eta$ of the resulting total gas mass and of the internal energy $U_0 = -\alpha_0(E_1 + E_2)/(1 + \alpha_0)$ would be dissipated, where $\alpha_0 = (M_{g1} + M_{g2})/(M_{*1} + M_{*2})$. The two schemes lead to identical predictions when $\alpha_1 = \alpha_2$, or, for $\alpha_1 \neq \alpha_2$, when $\sigma_1 = \sigma_2$.

[7] Note that the slopes of the three considered scaling laws are mutually consistent within the errors; that is, the combination of the FJ and Kormendy relations gives the adopted edge-on FP best fit. Similar results are obtained using the $K$-band relations of Pahre et al. (1998).

$[R_e \propto \sigma^{1.51} I_e^{-0.77}$, rms$(\log R_e) = 0.049]$ relations in the $z$ band as given by Bernardi et al. (2003a, 2003b); we also consider the $M_{\rm BH}$-$\sigma$ relation (Ferrarese & Merritt 2000; Gebhardt et al. 2000). An important issue of the present analysis is then how to map, for each galaxy model, the two sets $(M_*, r_v, \sigma_v)$ and $(L, R_e, \sigma)$.

Because we are not using $N$-body simulations, where under the assumption of a constant mass-to-light ratio $\Upsilon_*$ the relation between virial and "observed" properties is known (e.g., see NLC03), we adopt a conservative approach, and we assume a mass-dependent structural *weak homology* of our galaxies compatible with the FP tilt (e.g., see BCD02): in practice, we "force" the models to stay on the edge-on FP, and then we check if and how the FJ and Kormendy relations are preserved. This assumption is well founded, both observationally and theoretically. In fact, it is known that the edge-on FP is characterized by a tilt; that is, by a systematic trend of the ratio between the stellar mass-to-light ratio $\Upsilon_*$ and the virial parameter $K_v$,

$$\frac{\Upsilon_*}{K_v} \propto L^{-(\alpha+2\beta)/\alpha} R_e^{(2+\alpha+4\beta)/\alpha}, \tag{20}$$

where $GM_* = K_v R_e \sigma^2$, and the identity above holds for the general expression of the edge-on FP, $\log R_e = \alpha \log \sigma + \beta \log I_e + \gamma$ (curiously, we note that while in the $B$ band all the tilt depends on luminosity, in the present case and in the $K$ band it is almost due only to $R_e$, with $\Upsilon_*/K_v \propto L^{0.02} R_e^{0.28}$; e.g., see Treu 2001, BCD02). Unfortunately, a definite answer about the origin and the physical driving parameter(s) of the FP tilt is still missing. It is, however, known that a structural weak homology could be able to produce the whole of (or a large part of) the FP tilt. In particular, Sérsic (1968) models provide a remarkably good description of the light profiles of elliptical galaxies (e.g., see Caon et al. 1993; Graham & Colless 1997), with the Sérsic index $n$ increasing with galaxy luminosity and spanning the range of values required by equation (20) to reproduce the FP tilt (e.g., see Ciotti et al. 1996; Ciotti & Lanzoni 1997; BCD02). Note that an increase of $n$ with galaxy mass was also found in $N$-body simulations of major mergers (NLC03). Thus, in this paper we introduce a weak homology by assuming that for a galaxy characterized by the pair $(r_v, \sigma_v)$, the observables $R_e$ and $\sigma$ are given by

$$\frac{r_v}{R_e} \simeq \frac{250.26 + 7.15n}{77.73 + n^2}, \tag{21}$$

$$\frac{\sigma}{\sigma_v} \simeq \frac{24.31 + 1.91n + n^2}{44.23 + 0.025n + 0.99n^2}. \tag{22}$$

The two relations above, where $\sigma$ is the luminosity-weighted projected velocity dispersion within $R_e/8$, hold with very good accuracy for one-component, isotropic Sérsic models with $2 \lesssim n \lesssim 12$ (Ciotti 1991; Ciotti & Lanzoni 1997; Ciotti & Bertin 1999). From equations (21) and (22), the corresponding virial coefficient $K_v(n) = (r_v/R_e)(\sigma_v/\sigma)^2$ is easily found (see also BCD02). How a specific value of $n$ is assigned to a given galaxy model is described in the following sections (§§ 2.2 and 3).

### 2.2. *Equal-Mass Merging*

In order to illustrate the effect of repeated dry and wet mergers on a population of elliptical galaxies, in this section we start our analysis by presenting the idealized case of a merging hierarchy of equal-mass spheroids, extending the analysis of CvA01 to the dissipative case. The seed galaxies (the zeroth-order generation) are identical systems characterized by a stellar mass $M_{*0}$, a gas mass $M_{g0} = \alpha_0 M_{*0}$, a central BH mass $M_{\rm BH0} = \mu_0 M_{*0}$, a virial radius $r_0$, and a virial velocity dispersion $\sigma_0$. A galaxy of the $i$th generation is the merger product of two galaxies of generation $i-1$, so the equations (10)–(19) can be written in recursive form. The solution of the gas mass from equation (12), which in the present case reads $M_{gi+1} = 2(1-\eta-f\eta)M_{gi}$, is

$$M_{gi} = (2q)^i M_{g0}, \quad q \equiv 1 - \eta - f\eta, \tag{23}$$

so for $q \leq 1/2$, the gas mass is a steadily decreasing quantity along the merging hierarchy. The stellar mass from equation (10) becomes $M_{*i+1} = 2M_{*i} + 2\eta M_{gi}$, and from equation (23) we obtain

$$M_{*i} = 2^i \left(1 + \alpha_0 \frac{1-q^i}{1+f}\right) M_{*0}, \tag{24}$$

while the gas-to-star mass fraction at stage $i$ is given by

$$\alpha_i = \frac{\alpha_0 q^i (1+f)}{1+f+\alpha_0(1-q^i)}; \tag{25}$$

at variance with $M_{gi}$, $\alpha_i$ is a decreasing function of $i$ independent of the value of $q$. In Figure 1 we show the evolution of $\alpha_i$ along sequences of 10 equal-mass mergers, starting from gas-dominated seed galaxies ($\alpha_0 = 4$), for different values of $\eta$ (with $f = 10^{-3}$): according to equation (24), the stellar mass increases by a factor of $\sim 10^3$ for $\eta = 0$ and of $\sim 5 \times 10^3$ for $\eta = 0.9$. The horizontal solid line at $\alpha_i = \alpha_0$ represents the dry merging case ($\eta = 0$; note that we call "wet" a merging in which gas dissipation is active: a gas-rich merger with $\eta = 0$ is in practice a dry merger). When significant dissipation is present, $\alpha_i$ dramatically decreases in the first mergers as the combined effects of gas depletion and the associated stellar mass increase. Only for values of $\eta$ as low as $\sim 0.1$ is a more gentle evolution produced.

The BH mass evolution from equation (11), $M_{{\rm BH}i+1} = 2^{1/p} M_{{\rm BH}i} + 2f\eta M_{gi}$, is solved with the aid of equation (23) and reads

$$M_{{\rm BH}i} = 2^{i/p} M_{\rm BH0} \times \begin{cases} 1 + \dfrac{f\eta\alpha_0}{\mu_0} \dfrac{2^{i(1-1/p)} q^i - 1}{q - 2^{1/p-1}}, & q \neq 2^{1/p-1}, \\ 1 + \dfrac{f\eta\alpha_0}{\mu_0} 2^{1-1/p} i, & q = 2^{1/p-1}; \end{cases} \tag{26}$$

the explicit formula of the BH-to-star mass ratio $\mu_i$ (eq. [14]) can be derived from equation (24) and the equation above. The evolution of $\mu_i$ is shown in the middle panel of Figure 1 for the maximally radiative case $p = 2$ and for a fixed $f = \mu_0 = 10^{-3}$; while the Magorrian relation is preserved by construction in the case of classical BH merging ($p = 1$; *solid horizontal line*), in the extreme ($p = 2$) case, $\mu_i$ decreases for increasing galaxy mass, even though fresh gas is added to the BH at each merging in proportion to the stellar mass increase. Thus, in order to preserve the Magorrian relation when $p > 1$, an increasing fraction $f\eta$ of the available gas must be accreted on the BH as the merging hierarchy proceeds, increasing the active galactic nucleus (AGN) activity. When the progenitor spheroids are gas-rich, high values of $\eta$ may initially compensate for the decrease of $\mu$ due to

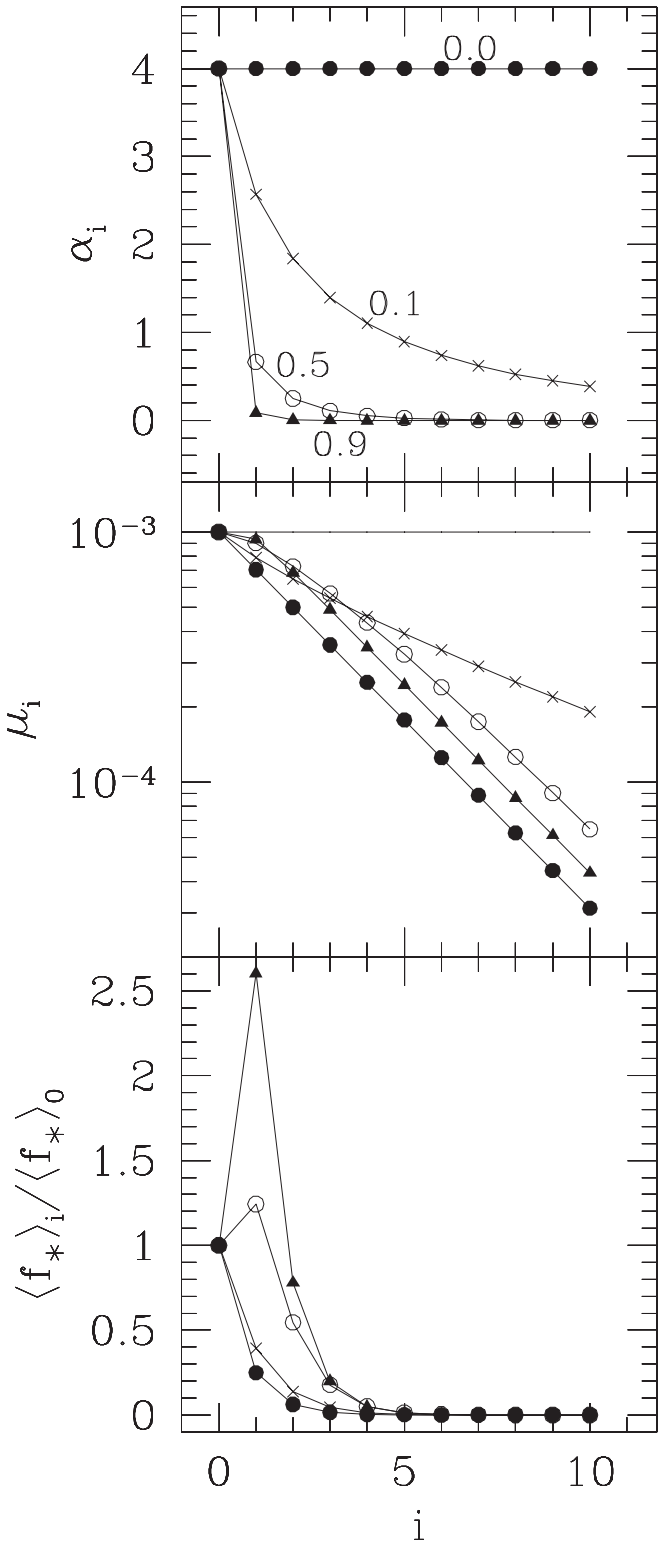


FIG. 1.—Evolution of the gas-to-star mass ratio $\alpha_i$ (*top*), the BH-to-star mass ratio $\mu_i$ (*middle*), and the stellar mean phase-space density $\langle f_* \rangle_i \equiv \langle \rho_* \rangle_i / \sigma_{vi}^3$ (*bottom*) in the case of 10 successive equal-mass parabolic mergers, for different values of the dissipation parameter $\eta$ (0, *filled circles*; 0.1, *crosses*; 0.5, *open circles*; 0.9, *triangles*). In all the merging sequences, $\alpha_0 \equiv M_{g0}/M_{*0} = 4$ and $f = \mu_0 = 10^{-3}$. Maximum radiative efficiency ( $p = 2$) is assumed for the BH coalescence law in the middle panel (the $p = 1$ case is represented by the horizontal line).

gravitational radiation; however, after a few mergers these galaxies run out of gas, and the final values of $\mu$ are even lower than those in the less dissipative $\eta = 0.1$ case.

From equations (16) and (17) we finally obtain the relations between the virial velocity dispersion and the virial radius of the progenitors and of the new galaxy:

$$\frac{\sigma_{vi}^2}{\sigma_{vi-1}^2} = 1 + \frac{\eta(1+2f)\alpha_{i-1}}{1+(1-f\eta)\alpha_{i-1}}, \tag{27}$$

$$\frac{r_{vi}}{r_{vi-1}} = \frac{2[1+(1-f\eta)\alpha_{i-1}]^2}{(1+\alpha_{i-1})[1+\alpha_{i-1}+\eta(1+f)\alpha_{i-1}]}. \tag{28}$$

As expected, $\sigma_v$ is larger (and $r_v$ is smaller) in the wet than in the dry merging case; for example, $\sigma_{vi}^2 \sim \sigma_{vi-1}^2(1+\eta)$ and $r_{vi} \sim 2r_{vi-1}/(1+\eta)$ in the limit of $\alpha_{i-1} \gg 1$. Figure 1 shows how gas dissipation may produce a nonmonotonic behavior of the quantity $\langle f_* \rangle_i \equiv \langle \rho_* \rangle_i / \sigma_{vi}^3 = 3M_{*i}/(8\pi r_{vi}^3 \sigma_{vi}^3)$, which is often considered an estimate of the phase-space density. In particular, while $\langle f_* \rangle_i$ decreases as $\langle f_* \rangle_0 / 4^i$ in equal-mass dry merging, in highly dissipative gas-rich mergers, the increase of $\langle \rho_* \rangle$ dominates over the increase of $\sigma_v^3$, and

$$\langle f_* \rangle_i \sim \langle f_* \rangle_{i-1}(1+\eta\alpha_{i-1})(1+\eta)^{3/2}/4.$$

From the previous formula, one would then conclude that an increase of the phase-space density is limited to exceptionally gas-rich mergers, but this is not correct. In fact, $\langle f_* \rangle$ is based on virial quantities that by their nature refer to global scales: an increase of the phase-space density in the galactic central regions can be produced by the *localized* dissipation of a smaller amount of gas.

In Figure 2 we plot the representative points of the same models of Figure 1 in the $M_*$-$\sigma$, $M_*$-$R_e$, $M_*$-$R_e$-$\sigma$, and $M_{\rm BH}$-$\sigma$ planes. These plots, under the assumption of the same stellar mass-to-light ratio $\Upsilon_*$ for all models, correspond to the FJ (Fig. 2*a*), Kormendy (Fig. 2*b*), and FP (Fig. 2*c*) planes. The assumption of a constant value for $\Upsilon_*$ is made less severe by comparing the models to the observed scaling laws in the *z* band (*dotted lines*), where the metallicity effects on $\Upsilon_*$ are reduced with respect to bluer wavelengths. Merging-induced structural weak homology is imposed by assuming that the seed galaxies are Sérsic $n = 2$ models, in accordance with the observed light profiles of low-luminosity elliptical galaxies, and that $n$ increases by 1 in each merging, as shown by numerical simulations (NLC03). In this way, the final range of values spanned by $n$ is between 2 and 12, consistent with observations. In practice, for assigned values of $r_0$ and $\sigma_0$ of the seed galaxies, from equations (21) and (22), with $n = 2$, we obtain their values of $R_e$ and $\sigma$. We also assume that the seed galaxies are placed at the lower end of the various scaling laws represented in Figure 2. The equal-mass merging formula given in equations (27)–(28) is then applied, and the new virial radius and velocity dispersion are mapped to the corresponding $R_e$ and $\sigma$ again from equations (21) and (22) with $n = 3$, and so on.

From Figure 2*c* it is apparent how the FP tilt is well reproduced by the models corresponding to dry mergers (*filled circles*). The adopted prescription for weak homology is relevant here: in fact, it is easy to prove that if the models were plotted by using $r_v$ and $\sigma_v$ instead of the fiducial $R_e$ and $\sigma$, they would be placed along a line of slope $-1/\beta \sim 1.3$ (for a surface brightness coefficient of $\beta = -0.77$ in the FP expression) instead of 1. Figure 2*c* also shows that highly dissipative wet mergers are initially displaced from the FP, but they again move along lines

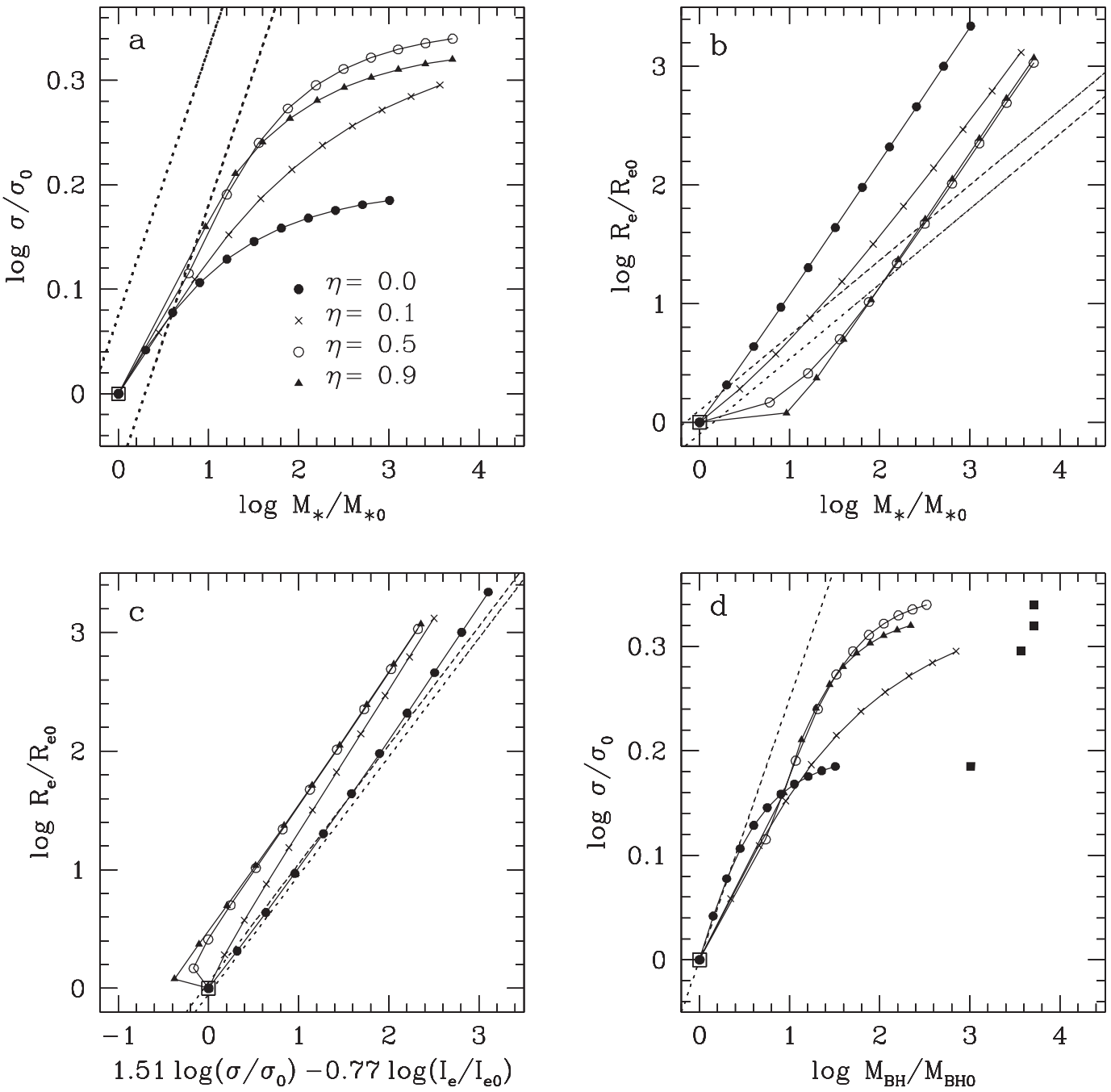


FIG. 2.—Models of Fig. 1, shown in the scaling relation planes. Dotted lines in panels ($a$–$c$) represent the observed scaling relations in the $z$ band with their 1 rms scatter. In panel $d$, the $M_{\rm BH}$-$\sigma$ relation is plotted without scatter, and $p = 2$ is assumed for the BH coalescence formula, while filled squares mark the position of the last merger product if $p = 1$. See § 2.2 for details.

almost parallel to the edge-on FP as soon as a large fraction of gas is converted into stars. These simple considerations indicate that the final position of a galaxy in the FP space after merging is sensitive to the physical processes involved, as already discussed by Bender et al. (1993). At variance with the edge-on FP, neither the FJ nor the Kormendy relations are reproduced: in particular, while the velocity dispersions are too low, the effective radii are too large. Again, note that this inconsistency would be exacerbated when plotting $r_v$ and $\sigma_v$; for example, the filled circles in Figure 2*a* would be aligned on a horizontal line, while in Figure 2*b* they would be placed on the line $r_v \propto M_*$. From Figure 2*d* it is finally apparent how the $M_{\rm BH}$-$\sigma$ relation has also failed, especially in the classical merging case. Remarkably, for $p = 2$, the mass loss due to emission of gravitational waves maintains the BH mass nearer to the observed relations than the classical merging case. In general, wet mergers are in better agreement with the FJ and Kormendy relations than are the dry mergers (in a way dependent on the specific value of $\eta$), due to the shrinking of $r_v$ and the increase of $\sigma_v$. Unfortunately, in the present framework we cannot evaluate the galaxy nonhomology induced by gas dissipation, which can be investigated only with $N$-body + gas numerical simulations such as those of Robertson et al. (2006a), and so weak homology is just imposed with the same prescription as for dry mergers. In any case, the preliminary analysis of this section is consistent with the idea that the FJ and Kormendy relations are stronger tests for merging than the edge-on FP, as

has already been clearly shown by numerical simulations (e.g., see NLC03; Boylan-Kolchin et al. 2005, 2006).

## 3. THE SIMULATIONS

In this section we extend the previous investigation to the study of the effects of repeated parabolic merging on a *population* of elliptical galaxies. The merging spheroids are extracted by means of Monte Carlo simulations from different samples of seed galaxies, and the properties of the resulting galaxies are determined by using the relations derived in § 2. The motivation for these simulations is the fact that equal-mass merging maximizes (minimizes) the effects on the radius (velocity dispersion) of the resulting objects, while mergers of galaxies spanning a substantial range of masses, sizes, and velocity dispersions not only are more realistic, but also could lead to less dramatic effects on the scaling relations.

In particular, we focus on two schemes designed to explore and quantify the impact of dry and wet merging on the formation and evolution of elliptical galaxies. In the first scheme the seed galaxies span only a narrow mass range (a factor of $\sim$5); in this case we then study whether massive elliptical galaxies and the observed scaling relations can be *produced* by repeated mergers of low-mass spheroidal systems. In the second scheme the seed elliptical galaxies follow the observed scaling relations over their whole observed mass range ($\sim 10^3$), and so we explore whether repeated merging events preserve or destroy these relations. For the sake of completeness, and also to check the robustness of the results obtained with the Monte Carlo simulations, we finally conduct a third set of experiments in which the merging histories are described by Press & Schechter (1974) merger trees.

How the mass, virial radius, and velocity dispersion of the seed galaxies, as well as their effective radius and central velocity dispersion, are assigned in each experiment is described in the following sections. In all cases, however, the initial mass of the SMBH obeys the Magorrian relation with $\mu_0 = 10^{-3}$.

### 3.1. *Merging Small Seed Galaxies*

In this first scheme, once two spheroids are extracted from the initial population (made of 1000 objects), they are merged together, and the properties of the merger end product are computed as described in § 2. The two progenitors are then removed from the seed galaxy population, while the new object is added to it; the procedure is repeated until the largest produced galaxies are $\sim 10^3$ times more massive than the smallest seed galaxy in the original sample. This may require up to 10–12 mergers, $\sim$7–10 of which are major mergers (i.e., merging in which the stellar mass ratio of the progenitors is in the range 0.3–3; e.g., see Kauffmann et al. 1994). The initial population of seed galaxies is obtained by random extraction (with the von Neumann rejection technique) of the stellar mass $M_*$ from the Sloan Digital Sky Survey (SDSS) $z$-band galaxy luminosity function (Blanton et al. 2001), under the assumption of a constant stellar mass-to-light ratio $\Upsilon_*$. Finally, the mass ratio of the most massive to the least massive galaxy in the sample is taken to be 5. In the case of wet mergers, the *total* (stars + gas) mass is the quantity that is extracted. For each galaxy mass, the corresponding central velocity dispersion $\sigma$ is fixed according to the $z$-band FJ relation, and the effective radius $R_e$ is assigned from the FP relation in the $z$ band (Bernardi et al. 2003a, 2003b). Due to the restricted mass range, all the galaxies are assumed to be $n = 2$ Sérsic models, and so their virial radius $r_v$ and virial velocity dispersion $\sigma_v$ can be easily calculated. We then apply the rule that in major mergers the Sérsic index of the resulting galaxy is $n = 1 + \max(n_1, n_2)$, where $n_1$ and $n_2$ are the Sérsic indices of the progenitors. In minor mergers, the Sérsic index instead keeps the same value of the more massive galaxy. Note that this is a quite conservative assumption, because in NLC03 it was found that in head-on minor mergers $n$ actually *decreases*, producing galaxies that fall outside the edge-on FP.

Figures 3 and 4 show the results in the cases of dry ($\alpha_0 = 0$) and dissipative gas-rich ($\alpha_0 = 4$ and $\eta = 0.3$) parabolic merging, respectively; the mass interval spanned by the progenitors is indicated by the two vertical tick marks, the end product positions are represented by the dots, and the observed scaling laws are represented by the dotted lines. Figure 3 reveals that massive elliptical galaxies cannot be formed by parabolic dry mergers of low-mass spheroids only, because they would be characterized by exceedingly large values of $R_e$ and almost mass-independent values of $\sigma$, in agreement with the results of CvA01 and NLC03 and with the conclusions of § 2. In fact, when galaxies reach a mass that is $\sim$10 times larger than that of the largest seed galaxies, all of the seed galaxy population can be considered to be made of equal-mass objects, and the considerations of § 2.2 apply.

Figure 4 shows the results in the case of wet merging of gas-dominated ($\alpha_0 = 4$) galaxies. As expected, mergers with gas dissipation produce more realistic objects than dry mergings, and, remarkably, the observed scaling laws are satisfied (even though with a large scatter) by the new galaxies, up to a mass increase of a factor of $10^2$ with respect to the smallest seed galaxies. However, new galaxies characterized by a mass increase factor of $\gtrsim 10^2$ are mainly formed by mergers of gas-poor galaxies that have already experienced several mergers, and so they deviate from the observed scaling laws like the galaxies in Figure 3.

More quantitatively, the models plotted in Figure 3 deviate from the observed $M_{\rm BH}$-$\sigma$ and FJ relations by more than 1 $\sigma$ when their (logarithmic) mass increase is $\gtrsim$1.4 and $\gtrsim$2.4, respectively, where the larger mass value that is allowed for the FJ relation is due to its larger scatter. The mean gas-to-star mass ratio for the deviating models is $\alpha \lesssim 0.5$ (even though several models with a lower value of $\alpha$ are still consistent with the two relations considered). Quite obviously, these values depend on the initial amount of gas; for example, when starting with $\alpha_0 = 10$, the models are incompatible with the observed $M_{\rm BH}$-$\sigma$ relation for a logarithmic increase of the stellar mass of $\gtrsim$2.2 and for $\alpha \lesssim 0.3$. We note, however, that the populated region in the edge-on FP is reduced for increasing values of $\alpha_0$, as can be seen by comparing the model distributions in Figures 3 and 4.

This first exploration therefore reveals that parabolic merging of low-mass galaxies only is unable to produce elliptical galaxies obeying the observed scaling laws, even when allowing for structural weak homology in a way that is consistent with the edge-on FP. However, gas dissipation plays an important role in gas-rich merging, and, remarkably, the resulting elliptical galaxies appear to be distributed proportionally to the observed scaling relations, as long as enough gas is available. Quite obviously, the problem of the compatibility of the properties of such merger products with other key observations, such as the color-magnitude and the metallicity–velocity dispersion relations, and the increasing age of the spheroids with their mass (e.g., see Renzini 2006; Gallazzi et al. 2006) cannot be addressed in the framework of this paper.

### 3.2. *Merging "Regular" Galaxies*

In the second scheme, the masses of the seed galaxies span the full range covered by ordinary elliptical galaxies ($\sim 10^3$), and their characteristic size and velocity dispersion follow the observed scaling relations. The mass, effective radius, and central

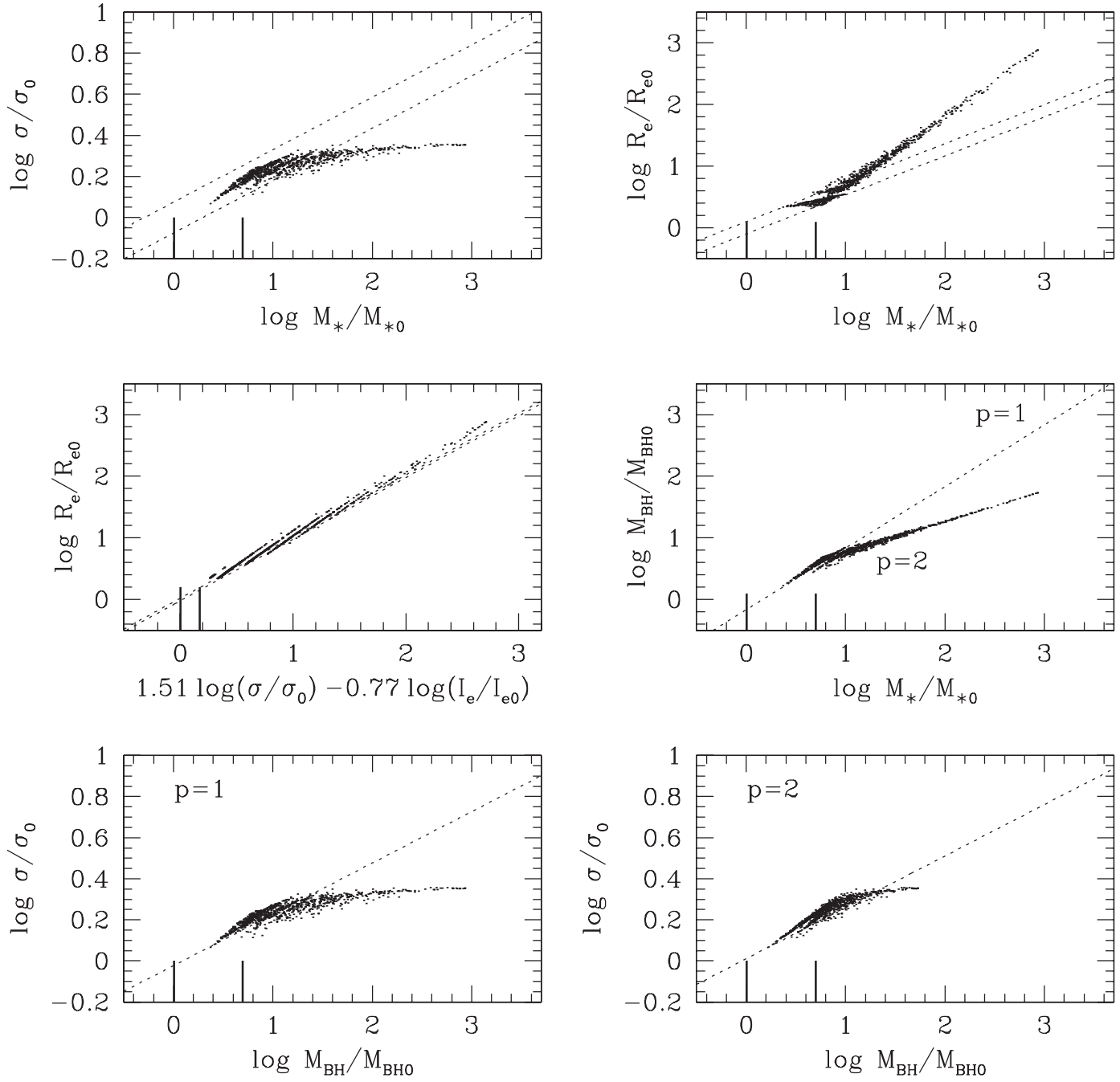


FIG. 3.—Synthetic scaling relations produced by parabolic dry mergers. Seed galaxies span a limited mass range (indicated by the heavy vertical tick marks), and random re-merging events are repeated until a factor of $10^3$ increase in mass is reached (see text for details). Dotted lines represent the observed scaling relations, as in Fig. 2. All quantities are normalized to the properties of the lowest mass seed galaxy.

velocity dispersion of each seed galaxy are assigned as described in § 3.1; however, due to the large mass range spanned in the present case, the models cannot be characterized by the same value of the Sérsic index, if they are placed on the edge-on FP. For this reason a Sérsic index is assigned to each seed galaxy by solving for $n$ the equation $K_v(n) = GM_*/R_e\sigma^2$; in turn, from the knowledge of $n$, we obtain the values of $r_v$ and $\sigma_v$ that are needed for the merging scheme. For simplicity, we restrict our study to major mergers only, increasing by 1 the larger Sérsic index characterizing each merging pair. Finally, for consistency with the imposed scaling laws (which hold for present-day gas-poor spheroids), we focus on dry merging only. In this section we then study the effect of merging on already established scaling laws.

In practice, once a galaxy is chosen, a second galaxy with a mass ratio relative to the first that is in the range 0.3–3 is extracted from the seed population, and then the two galaxies are merged. As in the other cases, the intrinsic galaxy properties are transformed into their "observational" counterparts by using equations (21) and (22). The procedure is repeated by selecting a third galaxy from the initial population, and so on for a total of six major mergers. The positions in the observational planes of 1000 galaxies (at all stages of the merging hierarchy) are shown in Figure 5. The main result is that now, at variance with the narrow mass range experiments, the scaling laws remain almost unaffected by the merging, both in their slope and in their scatter. In particular, note how the $M_{\rm BH}$-$\sigma$ relation (with $p = 2$) is preserved,

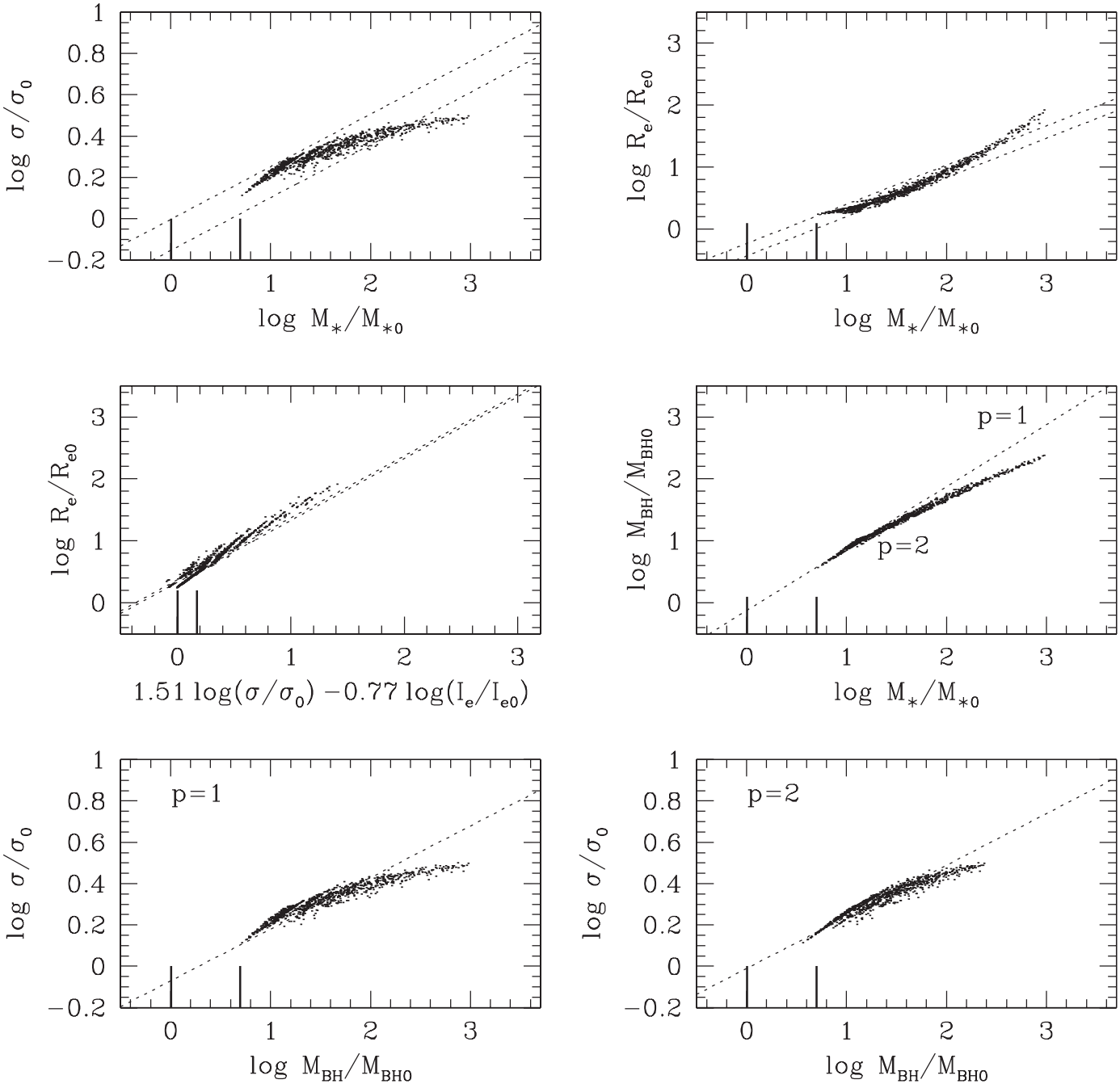


FIG. 4.—As in Fig. 3, but for the wet merging of initially gas-rich galaxies: $\alpha_0 = 4$ and $\eta = 0.3$.

even though we are in the dry-merging regime. The only detectable deviations from the observed scaling laws, for the same reasons already discussed in § 3.1, are found for elliptical galaxies with masses larger than the most massive galaxies in the original sample (marked by the two vertical tick marks in Fig. 5).

Why mergers do preserve the scaling relations so well? The reason is simple: by construction, in a population of galaxies that spans the whole mass range observed today and is distributed according to the observed scaling laws, mergers in general involve a "regular" elliptical galaxy, with realistic values of $R_e$ and $\sigma$. These mergings act as a "thermostat," maintaining values of $R_e$ in the observed range and increasing the virial velocity dispersion, thus contributing to the preservation of the scaling laws. Only when the produced galaxies are so massive that no regular galaxies of comparable mass are available do the new merger products deviate more and more from the scaling laws. This behavior becomes extreme in the case of repeated mergers in a galaxy population spanning a restricted mass range, as discussed in § 3.1. Thus, our analysis confirms that while the elliptical galaxy scaling laws (and so elliptical galaxies) cannot be produced by the merging of low-mass spheroids only (as already pointed out by, e.g., CvA01, NLC03, and Evstigneeva et al. 2004), these relations, once established by some other mechanism, are robust against merging.

### 3.3. *Cosmological Merger Trees*

We conclude our study by presenting a set of numerical experiments aimed at investigating the evolution of galaxies with a merging history obtained from the extended Press & Schechter (1974) formalism in a standard ΛCDM cosmology. The details

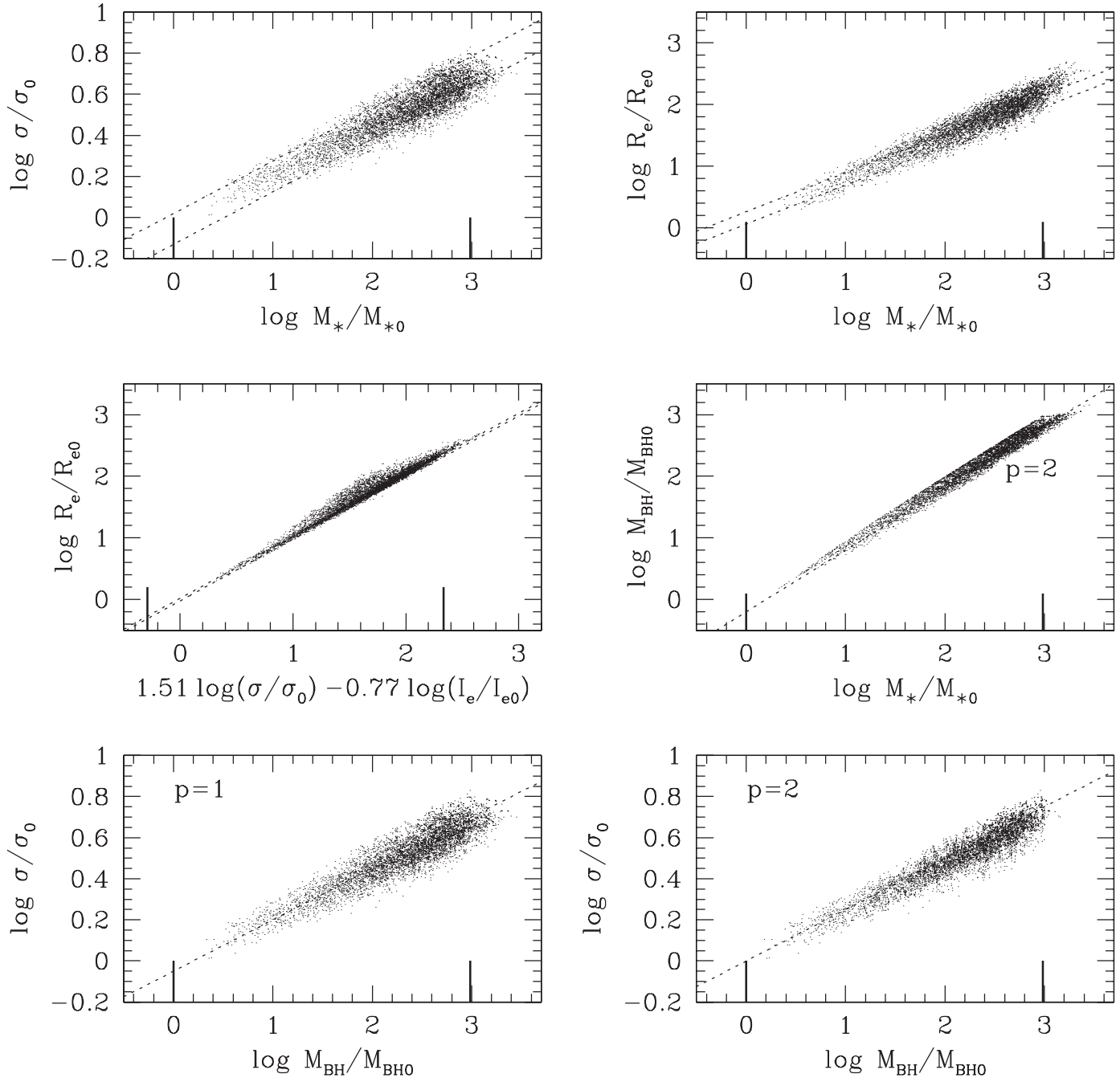


FIG. 5.—Synthetic scaling relations for the merger products of up to six dry major mergers of galaxies extracted from a population that follows the observed scaling laws. Lines are as in Fig. 2, and all quantities are normalized to the properties of the lowest mass seed galaxy.

of the realization of the merger trees are given in Volonteri et al. (2003), while the ensemble from which they have been extracted is in accordance with the modified Press-Schechter formula of Jenkins et al. (2001). In particular, we selected a set of 20 merger trees tracing the merger history, from $z = 5$ to $z = 0$, of a halo with mass $\simeq 10^{13}\ M_\odot$ at the present time. Since the mass resolution in the merger tree scales as $M_{\rm res} = 10^{10}(1+z)^{-3.5}\ M_\odot$, it follows that $M_{\rm res}$ is always $\lesssim$5% of the main halo mass in the merger hierarchy. This wide range of masses allows for both minor and major mergers in the tree at all redshifts.

In practice, we applied at each merging event in a given tree the relations derived in § 2, for both the dry and the wet ($\alpha_0 = 4$, $\eta = 0.3$) cases, for a total of 40 simulations. The virial radius $r_v$ of each seed halo (which we arbitrarily identify with a galaxy) is now defined as the radius of the sphere characterized by the mean mass density $\Delta_{\rm vir}\rho_{\rm crit}$ (where $\rho_{\rm crit}$ is the critical density for closure at redshift $z$, and $\Delta_{\rm vir}$ is the density contrast at virialization[8]). This definition of virial radius is not, strictly speaking, identical to the standard dynamical relation given in equation (9). However, in Lanzoni et al. (2004) it was shown that the two definitions of $r_v$ are in nice agreement, and so we also define the halo (galaxy) virial velocity dispersion from the virial theorem, $GM = r_v\sigma_v^2$. The properties of the merger end product are determined according to the dry or wet relations, while those of the secondary galaxy involved in each subsequent event follow the cosmological

[8] For the assumed cosmology, this can be approximated by $\Delta_{\rm vir} \simeq 178\Omega^{0.45}$ (Eke et al. 1998).

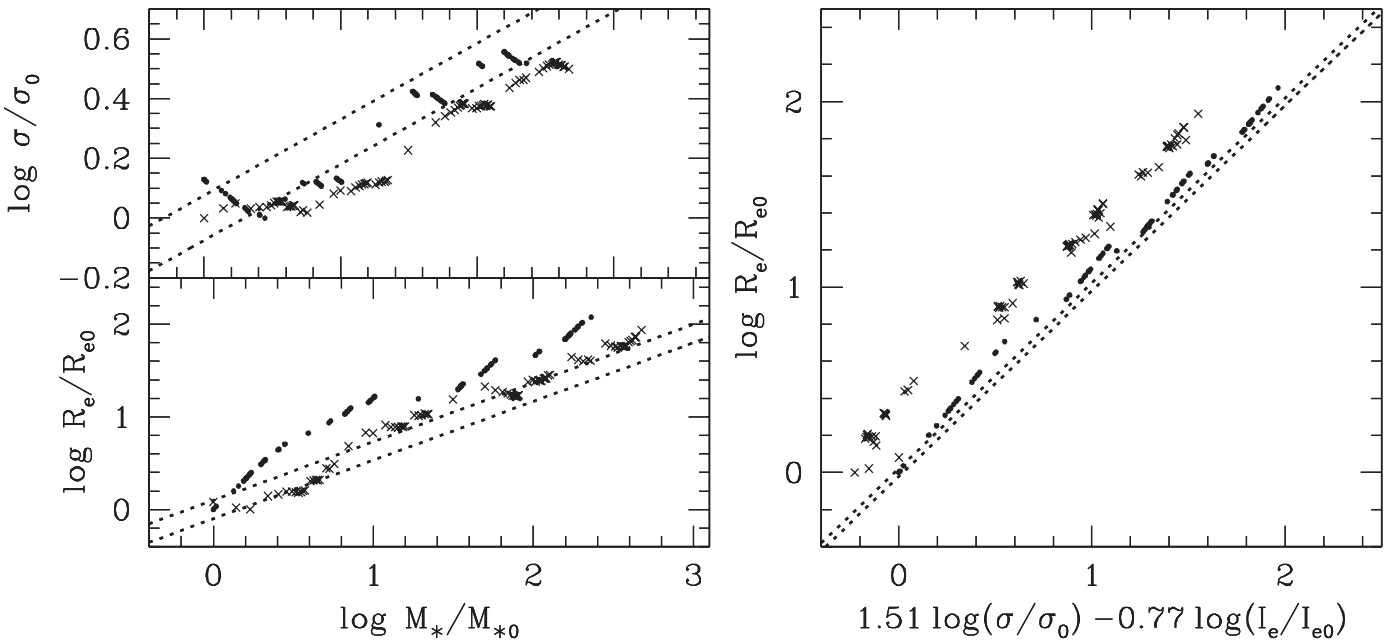


FIG. 6.—Evolutionary sequences of a main halo in the scaling law planes, according to a Press-Schechter merger tree, in the dry (*circles*) and wet ($\alpha_0 = 4$ and $\eta = 0.3$; *crosses*) cases.

virial relations. The weak homology trend is added to the models by assigning a Sérsic index of $n = 2$ to the main halo at $z = 5$ (which is assumed to be placed on the reference scaling laws) and increasing it by 1 in each major merger; in minor mergers, $n$ remains constant.

For simplicity, in Figure 6 we show the FJ, Kormendy, and FP planes for just 2 out of the 40 simulations, since the behavior of the galaxy models in all the merger trees is almost identical. Note that, at variance with Figures 3, 4, and 5, here the points constitute an evolutionary sequence, representing the successive positions of the main halo during its mass accretion history. From the comparison with Figures 3 and 4, it is apparent that deviations from the slope of the FJ and Kormendy relations are less strong than in the previous cases, while the evolutionary tracks of the growing halos move parallel to the edge-on FP plane.

The fact that in the merger tree exploration the slopes of the FJ, Kormendy, and FP relations are also preserved is not surprising, as it is easily explained when combining the results of previous sections with the fact that now the "galaxies" involved in the mergings are provided by the cosmological setting, in which $M \propto r_v^3 \propto \sigma_v^3$. Thus, the determining factor of success is again the availability of galaxies with a virial radius and velocity dispersion that increases with the halo mass, a property that cannot be produced by parabolic mergings of small systems only, but that is the natural consequence of the substantially different phenomenon of negative energy collapses (see § 1).

Note that the accordance with observations would be in fact even better than the results shown in Figure 6. According to the hierarchical merging picture, the number of mergers that an elliptical galaxy experiences in its lifetime (efficient mergers; i.e., those with timescales shorter than the Hubble time) is much smaller than the number of halo mergers in a cosmological merger tree, as only a small fraction ($\lesssim$30%) of them lead to galaxy mergers once the finite time needed for merging is taken into account (see Fig. 7). In fact, dynamical friction appears to be very efficient (i.e., with a decay timescale shorter than the Hubble time) only for mergers with a mass ratio of the progenitors that is $\gtrsim$0.1 (Taffoni et al. 2003), while satellites in the intermediate mass ratio range (0.01–0.1) suffer severe mass losses from the tidal perturbations induced by the gravitational field of the primary halo, and this progressive mass loss further increases the decay time. The lightest satellites are almost unaffected by orbital decay, so they survive and keep orbiting on rather circular, peripheral orbits.

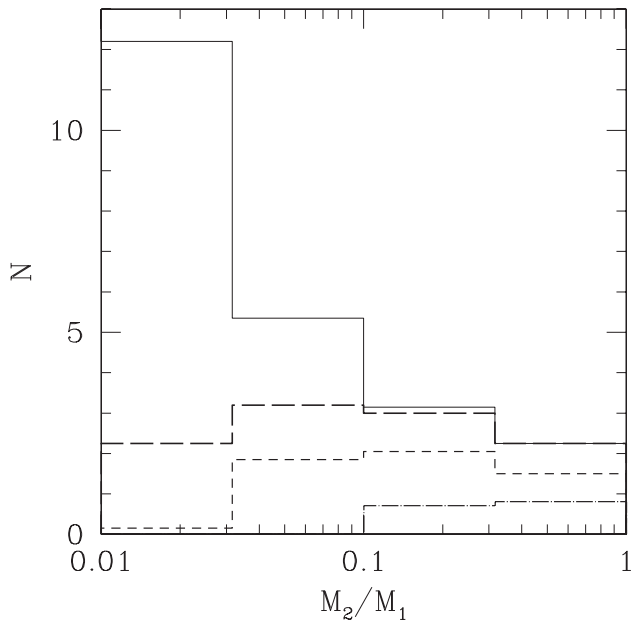


FIG. 7.—Number of mergers per logarithmic secondary-to-primary mass ratio, extracted from the merger history of a $M_0 = 10^{13}\ M_\odot$ halo at $z = 0$ and averaged over 20 merger trees. The total number of mergers experienced by the halo at $z < 3$ is shown by the solid histogram. The number of *efficient* mergers (see text for the definition) experienced by the same halo at a different redshift is shown by the long-dashed ($z < 3$), short-dashed ($z < 2$), and dot-dashed ($z < 1$) histograms.

## 4. DISCUSSION AND CONCLUSIONS

With the aid of a scheme based on very simple physical arguments, we investigated the influence of dry and wet merging on the formation and evolution of elliptical galaxies, focusing on the origin and robustness of some of their scaling laws. In particular, by using analytical arguments and numerical simulations, we showed that massive elliptical galaxies cannot be formed by (parabolic) merging of low-mass spheroidal galaxies, even in the presence of substantial gas dissipation and allowing for the helpful effects of structural weak homology. However, the observed scaling laws of elliptical galaxies, once established by galaxy formation, are robust against merging. More specifically, our findings can be summarized as follows:

1. Parabolic dry merging in a population of low-mass spheroids leads to massive elliptical galaxies that cannot be simultaneously placed on the Kormendy, FJ, and edge-on FP relations. For example, if we force the end products to stay on the edge-on FP, massive galaxies fail the FJ and Kormendy relations, with deviations increasing with galaxy mass. This behavior was predicted in CvA01 and confirmed by high-resolution numerical simulations (NLC03; Boylan-Kolchin et al. 2005, 2006). For example, Boylan-Kolchin et al. (2006), in a series of dissipationless merging simulations of galaxies in cosmologically motivated orbits, found that the merging end products, while preserving the edge-on view of the FP, can present significant differences in the FJ and Kormendy relations. This is because the variations in the resulting $M_*$-$R_e$ relation are compensated by corresponding variations in the $M_*$-$\sigma$ relation, so that the *projections* of the FP, but not the edge-on FP itself, should provide a powerful way to investigate the assembly history of massive elliptical galaxies.

2. Parabolic wet merging in the same population of low-mass progenitors leads to galaxies that are in much better agreement with the observed scaling relations, as long as enough gas for dissipation is available. In particular, the resulting $M_{\rm BH}$-$\sigma$ relation is in better agreement with the observed one, as is also true in the case of significant mass loss (via gravitational waves) of the coalescing BHs. Significant deviations from the observed scaling laws are, however, expected for massive galaxies. Similar conclusions were reached by sophisticated *N*-body plus hydrodynamic simulations of merging of disk galaxies. For example, Kazantzidis et al. (2005) found that merging disk galaxies constructed to obey the $M_{\rm BH}$-$\sigma$ relation move relative to it depending on whether they undergo a dissipational or dissipationless merger. In particular, remnants of dry mergings tend to move away from the mean relation, showing the role of gas-poor mergers as a possible source of scatter. In addition, Robertson et al. (2006b) studied the development of the $M_{\rm BH}$-$\sigma$ relation over cosmic time with a large set of hydrodynamic simulations of galaxy mergers that include star formation and feedback from the growth of the central BH, and they found that the $M_{\rm BH}$-$\sigma$ relation is created through coupled BH and spheroid growth (via star formation) in galaxy mergers.

3. Parabolic dry mergers in a population of galaxies following the observed scaling laws over the full mass range populated today by stellar spheroids (or following the scaling laws of dark matter halos predicted by the current cosmological scenario) preserve the Kormendy, FJ, and edge-on FP relations remarkably well. The reason for this behavior is rooted in the availability of the merger population of galaxies with velocity dispersion increasing with galaxy mass. Remarkably, Robertson et al. (2006a) found evidence that dry merging of spheroidal galaxies at low redshift is expected to maintain the FP relation *imprinted by gas-rich merging during the epoch of rapid spheroid and central BH growth at high redshift*, when the progenitors were characterized by gas fractions of $\gtrsim$30% and efficient gas cooling was allowed in the simulations.

Thus, points 1 and 2 above suggest that elliptical galaxies cannot be originated by parabolic merging of low-mass spheroids only, even in the presence of substantial gas dissipation. In addition, point 3, when considered together with the cosmologically imprinted scaling laws of dark matter halos and the several appealing features of dissipationless collapse end products (see § 1), supports the idea that elliptical galaxies formed in a process similar to monolithic collapse, even though their structural and dynamical properties are compatible with a limited number of dry mergers (we note that the same conclusion has also been reached from the study of color profiles in early-type galaxies, as described in Wu et al. 2005).

The possibility that monolithic collapse and successive merging are just the leading physical processes at different times in galaxy evolution, and that they are both important for galaxy formation, is perhaps indicated also by a "contradictory" and often overlooked peculiarity of massive elliptical galaxies. In fact, while the Kormendy relation dictates that the mean stellar density of galaxies decreases for increasing galaxy mass (a natural result of parabolic dry merging), the normalized light profiles of elliptical galaxies becomes steeper and their metallicity increases with increasing galaxy mass (as expected in the case of significant gas dissipation). Thus, the present-day light profiles of elliptical galaxies could represent the fossil evidence of the impact of both of the processes; quite obviously, this problem cannot be addressed in the framework adopted in this paper. It would be very interesting to extend the Robertson et al. (2006a) and Naab et al. (2007) analysis to the study of dissipative collapses in cosmologically motivated dark matter halos, thus extending the investigation of Nipoti et al. (2006) toward the very early phases of galaxy formation.

We thank the anonymous referee for useful comments that improved the presentation of the paper. L. C. acknowledges the warm hospitality of the Theoretical Astrophysics Division of Harvard-Smithsonian Center for Astrophysics, where a large part of this work was carried out. Lars Hernquist, Jerry Ostriker, Brant Robertson, and Tjeerd van Albada provided insightful comments. L. C. is supported by MIUR grant CoFin2004.

## REFERENCES

Aguilar, L. A., & Merritt, D. 1990, ApJ, 354, 33
Almeida, C., Baugh, C. M., & Lacey, C. G. 2007, MNRAS, in press (astro-ph/0608544)
Bell, E. F., et al. 2004, ApJ, 608, 752
———. 2006, ApJ, 640, 241
Bender, R., Burstein, D., & Faber, S. M. 1993, ApJ, 411, 153
Benson, A. J. 2005, MNRAS, 358, 551
Bernardi, M., et al. 2003a, AJ, 125, 1849
———. 2003b, AJ, 125, 1866
Bernardi, M., et al. 2003c, AJ, 125, 1882
Bertin, G., Ciotti, L., & Del Principe, M. 2002, A&A, 386, 149 (BCD02)
Blanton, M. R., et al. 2001, AJ, 121, 2358
Bower, R. G., Lucey, J. R., & Ellis, R. S. 1992, MNRAS, 254, 589
Boylan-Kolchin, M., Ma, C.-P., & Quataert, E. 2005, MNRAS, 362, 184
———. 2006, MNRAS, 369, 1081
Burkert, A., & Silk, J. 2001, ApJ, 554, L151
Burstein, D., Bender, R., Faber, S., & Nolthenius, R. 1997, AJ, 114, 1365
Caon, N., Capaccioli, M., & D'Onofrio, M. 1993, MNRAS, 265, 1013

Capelato, H. V., de Carvalho, R. R., & Carlberg, R. G. 1995, ApJ, 451, 525
Cavaliere, A., & Vittorini, V. 2002, ApJ, 570, 114
Ciotti, L. 1991, A&A, 249, 99
Ciotti, L., & Bertin, G. 1999, A&A, 352, 447
Ciotti, L., & Lanzoni, B. 1997, A&A, 321, 724
Ciotti, L., Lanzoni, B., & Renzini, A. 1996, MNRAS, 282, 1
Ciotti, L., & van Albada, T. S. 2001, ApJ, 552, L13 (CvA01)
Conselice, C. J. 2006, ApJ, 638, 686
Dantas, C. C., Capelato, H. V., Ribeiro, A. L. B., & de Carvalho, R. R. 2003, MNRAS, 340, 398
Dekel, A., & Cox, T. J. 2006, MNRAS, 370, 1445
de Vaucouleurs, G. 1948, Ann. d'Astrophys., 11, 247
de Zeeuw, P. T. 2001, in Black Holes in Binaries and Galactic Nuclei: Diagnostics, Demography and Formation, ed. L. Kaper, E. P. J. van den Heuvel, & P. A. Woudt (Berlin: Springer), 78
Djorgovski, S., & Davis, M. 1987, ApJ, 313, 59
Dressler, A., Lynden-Bell, D., Burstein, D., Davies, R. L., Faber, S. M., Terlevich, R., & Wegner, G. 1987, ApJ, 313, 42
Eggen, O. J., Lynden-Bell, D., & Sandage, A. R. 1962, ApJ, 136, 748
Eke, V. R., Navarro, J. F., & Frenk, C. S. 1998, ApJ, 503, 569
Evstigneeva, E. A., de Carvalho, R. R., Ribeiro, A. L., & Capelato, H. V. 2004, MNRAS, 349, 1052
Evstigneeva, E. A., Reshetnikov, V. P., & Sotnikova, N. Ya. 2002, A&A, 381, 6
Faber, S. M., & Jackson, R. E. 1976, ApJ, 204, 668
Faber, S. M., et al. 2005, ApJ, submitted (astro-ph/0506044)
Ferrarese, L., & Merritt, D. 2000, ApJ, 539, L9
Ferrarese, L., van den Bosch, F. C., Ford, H. C., Jaffe, W., & O'Connell, R. W. 1994, AJ, 108, 1598
Gallazzi, A., Charlot, S., Brinchmann, J., & White, S. D. M. 2006, MNRAS, 370, 1106
Gebhardt, K., et al. 2000, ApJ, 539, L13
González-García, A. C., & van Albada, T. S. 2003, MNRAS, 342, L36
Graham, A., & Colless, M. 1997, MNRAS, 287, 221
Graham, A. W., Erwin, P., Trujillo, I., & Asensio Ramos, A. 2003, AJ, 125, 2951
Graham, A. W., & Guzmán, R. 2003, AJ, 125, 2936
Guzmán, R., Lucey, J. R., Carter, D., & Terlevich, R. J. 1992, MNRAS, 257, 187
Haehnelt, M. G., & Kauffmann, G. 2000, MNRAS, 318, L35
Haiman, Z., Ciotti, L., & Ostriker, J. P. 2004, ApJ, 606, 763
Hozumi, S., Burkert, A., & Fujiwara, T. 2000, MNRAS, 311, 377
Hughes, S. A., & Blandford, R. D. 2003, ApJ, 585, L101
Jenkins, A., Frenk, C. S., White, S. D. M., Colberg, J. M., Cole, S., Evrard, A. E., Couchman, H. M. P., & Yoshida, N. 2001, MNRAS, 321, 372
Jørgensen, I. 1999, MNRAS, 306, 607
Kauffmann, G., Guiderdoni, B., & White, S. D. M. 1994, MNRAS, 267, 981
Kazantzidis, S., et al. 2005, ApJ, 623, L67
Khochfar, S., & Burkert, A. 2003, ApJ, 597, L117
———. 2006, A&A, 445, 403
Khochfar, S., & Silk, J. 2006, MNRAS, 370, 902
Kormendy, J. 1977, ApJ, 218, 333
Lanzoni, B., Ciotti, L., Cappi, A., Tormen, G., & Zamorani, G. 2004, ApJ, 600, 640
Lauer, T. R., et al. 1995, AJ, 110, 2622
Londrillo, P., Messina, A., & Stiavelli, M. 1991, MNRAS, 250, 54
Magorrian, J., et al. 1998, AJ, 115, 2285
Matteucci, F. 1994, A&A, 288, 57
May, A., & van Albada, T. S. 1984, MNRAS, 209, 15
McGlynn, T. A. 1984, ApJ, 281, 13
McIntosh, D. H., et al. 2005, ApJ, 632, 191
Naab, T., Johansson, P. H., Ostriker, J. P., & Efstathiou, G. 2007, ApJ, in press (astro-ph/0512235)
Naab, T., Khochfar, S., & Burkert, A. 2006, ApJ, 636, L81
Nipoti, C., Londrillo, P., & Ciotti, L. 2003, MNRAS, 342, 501 (NLC03)
———. 2006, MNRAS, 370, 681
Oñorbe, J., Domínguez-Tenreiro, R., Sáiz, A., Artal, H., & Serna, A. 2006, MNRAS, 373, 503
Oñorbe, J., Domínguez-Tenreiro, R., Sáiz, A., Serna, A., & Artal, H. 2005, ApJ, 632, L57
Ostriker, J. P. 1980, Comments Astrophys., 8, 177
Pahre, M. A., Djorgovski, S. G., & de Carvalho, R. R. 1998, AJ, 116, 1591
Peebles, P. J. E. 1980, The Large-Scale Structure of the Universe (Princeton: Princeton Univ. Press)
Pentericci, L., Ciotti, L., & Renzini, A. 1996, Astrophys. Lett. Commun., 33, 213
Pipino, A., & Matteucci, F. 2004, MNRAS, 347, 968
Press, W. H., & Schechter, P. 1974, ApJ, 187, 425
Prugniel, P., & Simien, F. 1997, A&A, 321, 111
Renzini, A. 2006, ARA&A, 44, 141
Robertson, B., Cox, T. J., Hernquist, L., Franx, M., Hopkins, P. F., Martini, P., & Springel, V. 2006a, ApJ, 641, 21
Robertson, B., Hernquist, L., Cox, T. J., Di Matteo, T., Hopkins, P. F., Martini, P., & Springel, V. 2006b, ApJ, 641, 90
Saglia, R., Maraston, C., Greggio, L., Bender, R., & Ziegler, B. 2000, A&A, 360, 911
Sáiz, A., Domínguez-Tenreiro, R., & Serna, A. 2004, ApJ, 601, L131
Sérsic, J. L. 1968, Atlas de Galaxias Australes (Cordoba: Obs. Astron.)
Shen, S., Mo, H. J., White, S. D. M., Blanton, M. R., Kauffmann, G., Voges, W., Brinkmann, J., & Csabai, I. 2003, MNRAS, 343, 978
Taffoni, G., Mayer, L., Colpi, M., & Governato, F. 2003, MNRAS, 341, 434
Thomas, D., Greggio, L., & Bender, R. 1999, MNRAS, 302, 537
Tissera, P. B., Smith Castelli, A. V., & Scannapieco, C. 2006, A&A, 455, 135
Toomre, A. 1977, in Evolution of Galaxies and Stellar Populations, ed. B. M. Tinsley & R. B. Larson (New Haven: Yale Univ. Obs.), 401
Tremaine, S., et al. 2002, ApJ, 574, 740
Trenti, M., Bertin, G., & van Albada, T. S. 2005, A&A, 433, 57
Treu, T. 2001, Ph.D. thesis, Scuola Normale Superiore di Pisa
Trujillo, I., Erwin, P., Asensio Ramos, A., & Graham, A. W. 2004, AJ, 127, 1917
Udry, S. 1993, A&A, 268, 35
van Albada, T. S. 1982, MNRAS, 201, 939
van Dokkum, P. G. 2005, AJ, 130, 2647
Volonteri, M., Haardt, F., & Madau, P. 2003, ApJ, 582, 559
White, S. D. M., & Frenk, C. S. 1991, ApJ, 379, 52
Wu, H., Shao, Z., Mo, H. J., Xia, X., & Deng, Z. 2005, ApJ, 622, 244
Yu, Q., & Tremaine, S. 2002, MNRAS, 335, 965